STRUCTURE AND DIURNAL VARIATION OF THE ATMOSPHERIC BOUNDARY LAYER OVER A MID-LATITUDE GLACIER IN SUMMER

MICHIEL R. VAN DEN BROEKE *
Institute for Marine and Atmospheric Research PO Box 80.005, 3508 TA Utrecht, The Netherlands

(Received in final form 4 September, 1996)

Abstract. During the summer of 1994, a meteorological experiment (PASTEX) was performed over the Pasterze Glacier, Austria. In this paper we describe the average horizontal and vertical structure of the atmospheric boundary layer (ABL) above the melting glacier, as well as its diurnal variation during a period of fair weather. It was found that very persistent glacier winds with a vertical extent of 100 m dominate the summertime structure of the ABL, because the gravity force acting on the near surface air parcels is many times larger than the synoptic-scale pressure gradient. During fair weather, we find a well developed mountain-valley wind circulation above the katabatic layer. During daytime, the valley wind advects warm and humid air from the ice-free valley towards the glacier, limiting the development of the glacier wind. During the night, the downslope flows that develop above the ice-free valley walls (mountain wind) merge with the glacier wind and enhance the downslope transport of air. The associated subsidence is the most probable cause for the drying of the lower part of the atmosphere during the night. During periods of weak synoptic winds, the glacier wind effectively generates turbulence in the strongly stratified surface layer. On average, the turbulent fluxes of sensible and latent heat provide 25% of the total melting energy at the surface of the glacier tongue, and the influence of the glacier winds on the surface energy budget can therefore not be neglected.

1. Introduction

To study the interaction between the atmospheric boundary layer (ABL) and glacier melt, a glacio-meteorological experiment was performed on the Pasterze glacier in the Eastern Alps, Austria, during the summer of 1994 (PASTEX). During the last century, there has been a global sea level rise of approximately 15 cm (Warrick and Oerlemans, 1990) that can be largely attributed to the thermal expansion of sea water and the world-wide retreat of glaciers, owing to an estimated rise in near-surface air temperature of 0.66 ± 0.20 °C (Oerlemans and Fortuin, 1992; Oerlemans, 1994). For instance, the tongue of the Pasterze glacier has retreated more than 1.5 km during the past 150 years.

An outstanding feature of the glacier climate during PASTEX, and the main subject of the present paper, was the presence of very persistent glacier winds. Although the glacier wind is dynamically related to the katabatic winds over large ice sheets, and to nocturnal slope flows in mountainous areas (they are all gravity driven flows), the physical mechanism that causes them is quite different. The katabatic winds on the high parts of ice sheets and the nocturnal slope flows are

* *Present affiliation and corresponding address:* Norsk Polarinstitutt, Postboks 5072 Majorstua, N 0301 Oslo, Norway, e-mail: michiel@npolar.no.

Boundary-Layer Meteorology **83:** 183–205, 1997.

primarily caused by a radiation deficit at the surface (Parish and Waight, 1987). When the radiation balance at the surface becomes positive at daytime, the surface inversion and the associated slope flows disappear, and synoptic or mesoscale pressure gradients will determine the near surface winds (Kodama et al., 1989; Van den Broeke and Bintanja, 1995). When the large-scale flow is weak, anabatic (uphill) winds will develop.

The situation is very different for the melting zone of ice sheets and glaciers. During the summer, the surface energy balance of these ice masses is generally *positive*, but the surface temperature will not increase beyond the melting point of ice and will therefore remain lower than that of the overlying air. Cooling of the air layers near the melting ice surface forces the so-called glacier winds. According to Ohata (1989a), glacier winds are more persistent over large glaciers in a warm environment. Where they occur, they provide a lower threshold for the turbulent exchange between the atmosphere and the ice surface. Very persistent glacier winds have for instance been observed in the melting zone of the Greenland ice sheet (Van den Broeke et al., 1994a; Duynkerke and Van den Broeke, 1994) and above a large glacier in Patagonia (Ohata, 1989b). Especially on days with weak large-scale wind and strong warming of the surrounding terrain, the glacier wind effectively generates turbulence that would otherwise be absent in the (very) stable surface layer. Because the turbulent flux of sensible heat normally provides 10–40% of the melting energy, the influence of glacier winds on the climate sensitivity of ice masses might be an important one (Van den Broeke, 1996, 1997a) and glacier winds have received considerable attention from mass balance modellers (Hoinkes, 1954; Martin, 1975; Kuhn, 1978).

Stenning et al. (1981) discussed the influence of synoptic pressure gradients on glacier winds for Peyto Glacier, Canada, and found that the katabatic force was many times larger than the synoptic pressure gradient. Other papers deal with the detailed structure of the ABL over a melting glacier (Munro and Davies, 1977; Holmgren, 1971) and the application of surface-layer similarity theory in the glacier ABL (Munro and Davies, 1978; Munro, 1989). It is generally observed that glacier winds are very shallow, and that surface-layer similarity theory can only be applied in the lowest few metres of the ABL. Glacier winds in the eastern Alps have been documented at an early stage (Tollner, 1931; Tollner, 1935; Schwabl and Tollner, 1938; Tollner, 1952).

In this paper, we describe the average horizontal and vertical structure of the ABL over the Pasterze Glacier in summer. For a period of fair weather, we calculated the diurnal cycle of the different variables and discuss the interaction of the glacier wind and the mountain-valley wind system. We will also pay some attention to the influence of the glacier wind on the surface energy balance, although the detailed energy and mass balance measurements will be dealt with in a forthcoming paper. Another paper deals with the budgets of momentum, heat and moisture of the glacier wind layer (Van den Broeke, 1997b).

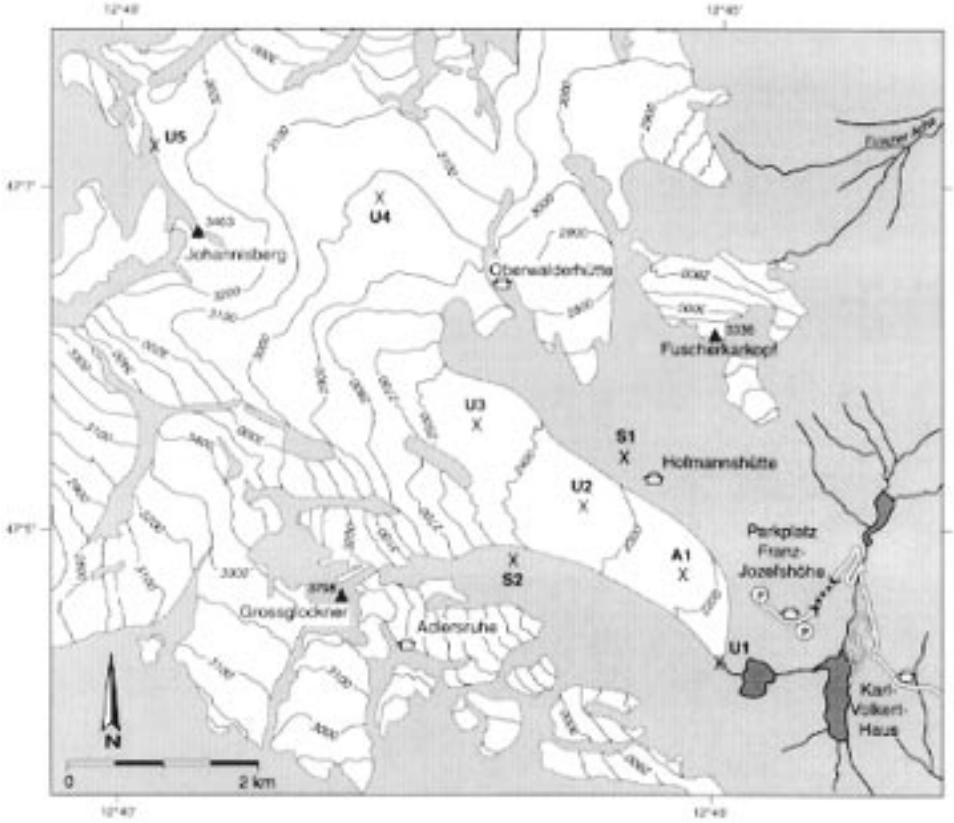

Figure 1. The Pasterze and surroundings. Masts are denoted by ×. White areas are glaciated, grey areas are rock surface.

2. Experimental Set-up

The Pasterze is the largest glacier of Austria, with a surface area of 19.8 km^2 and a length of 9.4 km (both in 1969, Bachmann, 1978). The general direction of the ice stream is north-west to south-east. During PASTEX, six masts stood along the centre streamline of the glacier (Figure 1), ranging in elevation from 2075 to 3225 m a.s.l. An ice fall marks the sudden transition from the accumulation area to the glacier tongue. Below and above the ice fall the surface slope is reasonably constant. The surface consisted mainly of snow above the ice fall and of bare ice at the glacier tongue.

At sites U1 to U5, we used meteorological masts with two measurement levels for temperature, wind speed and humidity (at 0.5 and 2 m) and one measurement level for the incoming and reflected shortwave radiation (1.5 m). Incoming long-wave radiation was measured at sites U2 and U5. U1 stood on bare soil just in front of the glacier, U2 and U3 were placed on the glacier tongue, U4 in the accumulation area not far above the ice fall and U5 at the ridge. At site A1, temperature, humidity

and wind were measured at 8 levels (0.25, 0.5, 1, 2, 4, 6, 8, 13 m). Every day at 12 GMT (14 LT), a cabled balloon sounded the lowest 500–1000 m of the atmosphere above the ice. During fair weather, the sounding frequency was intensified to once every three hours. The meteorological station Hoher Sonnblick (3106 m a.s.l.), approximately 20 km to the east of the Pasterze, provides a climatological background for the area with a temperature record that goes back to 1891. For a more detailed description of the experiment and the accuracy of the sensors, the reader is referred to Greuell et al. (1994).

3. General Meteorological Conditions During PASTEX

The experiment lasted from 15 June–16 August 1994, but for the present study we use data of the period 24 June–9 August (47 days), when all sensors worked synchronously. Unfortunately, owing to icing of the wind speed sensors and static electricity, some wind data are missing at sites U2, U4 and U5. The summer of 1994 was very warm over entire Western Europe; summer temperatures at Sonnblick were 2.2 K above the climatic mean. The eastern Alps were regularly under the influence of synoptic disturbances, which led to frequent occurrence of thunderstorms in the late afternoon.

3.1. A TYPICAL VERTICAL SOUNDING AT A1

Figure 2a–d shows the vertical distribution of temperature, specific humidity, wind speed and wind direction, typical for a fair summer day during PASTEX (23 July, 1625 LT). The glacier wind layer has some well-defined characteristics: the cooling effect of the melting glacier surface extends to about 100 m above the ice surface (Figure 2a); the maximum temperature of 14.5 °C is reached at about 20 m above the ice. This value is representative for the temperature above bare ground in the area surrounding the glacier. Thus, the lapse rate close to the glacier surface at daytime is typically 0.7 K m^{-1}. The cooling of the air near the glacier surface forces a well developed glacier wind, originating from 304°, to flow downslope with a wind speed maximum of 5.5 m s^{-1} at 6 m above the surface and a depth of approximately 100 m (Figure 2c). Changes in wind direction within the katabatic layer are very small, so variation of the cross slope wind speed with height does not contribute significantly to the wind shear (Figure 2d). Specific humidity is well mixed within the glacier wind layer, showing a rather constant value up to the level where the glacier wind disappears, where a sudden transition is observed towards higher values (Figure 2b). Note that the saturated specific humidity at the 0 °C ice surface equals approximately 5 g kg^{-1}, indicating downward transport of moisture at the surface (condensation).

Above the glacier wind layer, a valley wind is present with a strength of 2 m s^{-1} in a direction approximately opposite to the glacier wind. The valley wind advects

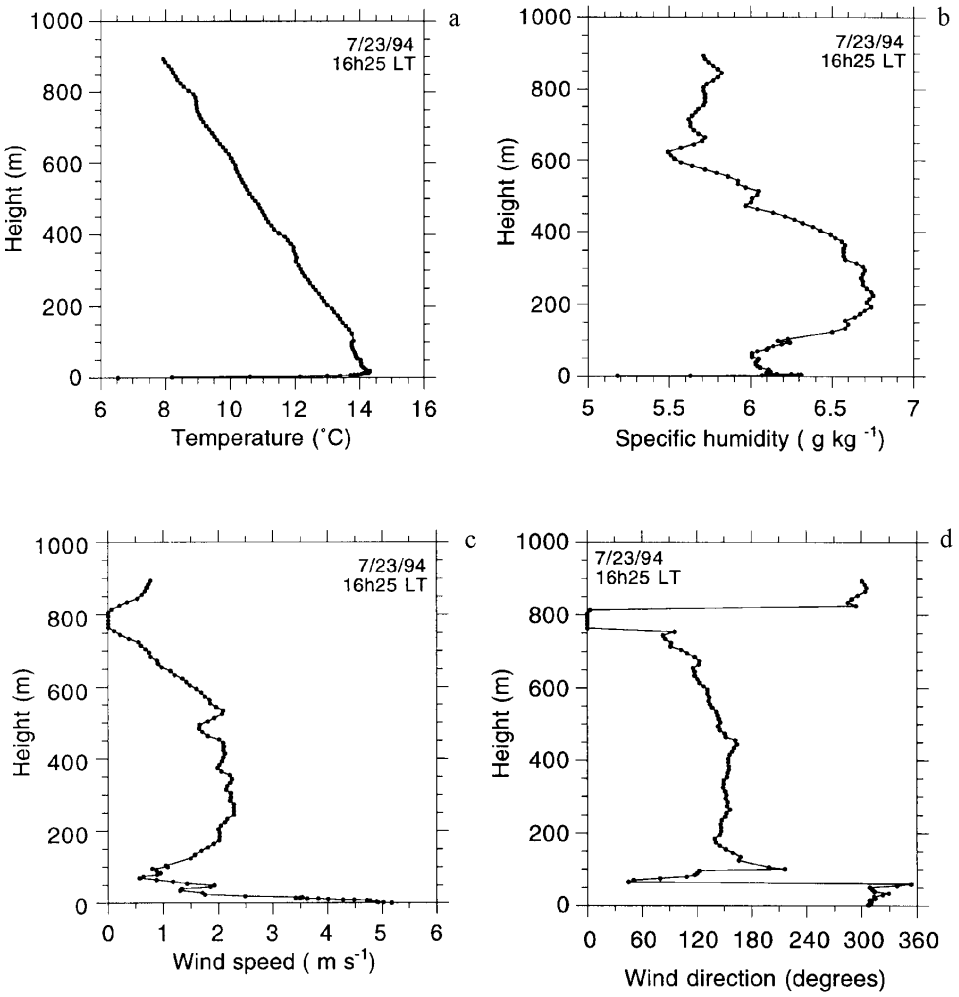

Figure 2. Vertical profiles of temperature (a), specific humidity (b), wind speed (c), and wind direction (d) at site A1, 23 June 1994, 1625 LT.

warm and humid air from the ice-free valley, thereby increasing the temperature and moisture contrast between the ambient atmosphere and the glacier surface. According to Figure 2c and d, the valley wind extends to 700–800 m above the glacier surface, above which the various variables approach their free atmosphere values. In the valley wind layer, the moisture is again well mixed and significantly higher values are found than in the glacier wind layer. We might conclude that the 'undisturbed' atmosphere overlying the glacier wind layer at daytime is in fact a near-neutral boundary layer that is advected from the valley floor. In section 4 we will discuss the diurnal variation of the local wind systems in more detail.

Table I

Surface elevation (h_s), average 2 m temperature (T_{2m}), potential temperature (θ_{2m}), specific humidity (q_{2m}), wind speed (V_{2m}) and wind directional constancy for the period 24 June–9 August 1994. Percentage between brackets indicates the amount of missing wind data.

Location	U1	A1	U2 (2%)	U3	U4 (4%)	U5 (13%)	Sonnblick
h_s (m a.s.l.)	2075	2205	2310	2420	2945	3225	3106
T_{2m} (°C)	7.3	6.8	6.4	7.1	3.7	3.4	5.5
θ_{2m} (K)	300.9	301.7	302.3	304.2	305.9	308.4	309.6
q_{2m} (g kg^{-1})	5.6	5.6	5.6	5.5	5.7	5.6	6.5
V_{2m} (m s^{-1})	3.7	4.1	4.4	4.5	4.0	3.9	3.5
dc	0.93	0.94	0.97	0.97	0.82	0.05	0.07

3.2. AVERAGE NEAR SURFACE VARIABLES

Average meteorological quantities at 2 m above the glacier surface (for the period 24 June to 9 August 1994) are listed in Table I. The wind directional constancy dc is defined as the ratio of vector averaged wind speed and average absolute wind speed during a certain period: dc = 1 indicates that the wind blows from one direction all the time, while dc = 0 indicates random wind directions. The directional constancy of the wind is normally used as a climatic quantity for a certain location, of which one or several years of data are available. On the shorter time scales of weeks to several months, however, the directional constancy proves to be a convenient parameter to detect local circulations. It should not be compared to the values that were presented by Wendler et al. (1993) for Antarctic katabatic winds, where dc has been calculated for several years of data.

The very high values of the directional constancy at the sites situated on or close to the glacier tongue (sites U1, A1, U2, U3 and U4) contrast sharply with those of the more exposed stations at site U5 and Sonnblick. This suggests that the near-surface flow at the glacier tongue is entirely gravity driven, its direction and strength determined by the glacier topography and the temperature contrast between the ABL and the ambient atmosphere. This is confirmed by the wind direction frequency distribution at various stations (Figure 3b–d): the dominant peaks in wind direction for the sites on the glacier tongue are all in the direction of the local glacier slope, and do not show a correlation with the distribution of the geostrophic wind direction at 500 hPa in Figure 3a. A peculiar feature is that at site U3, just below the ice fall, the absolute temperature (but not the potential temperature) and wind speed have a local maximum (Table I). In Section 4.1 it is suggested that this is caused by the interaction of the glacier wind with the mountain-valley wind system. The potential temperature decreases monotonically when the air flows down the glacier surface, indicating cooling at the surface.

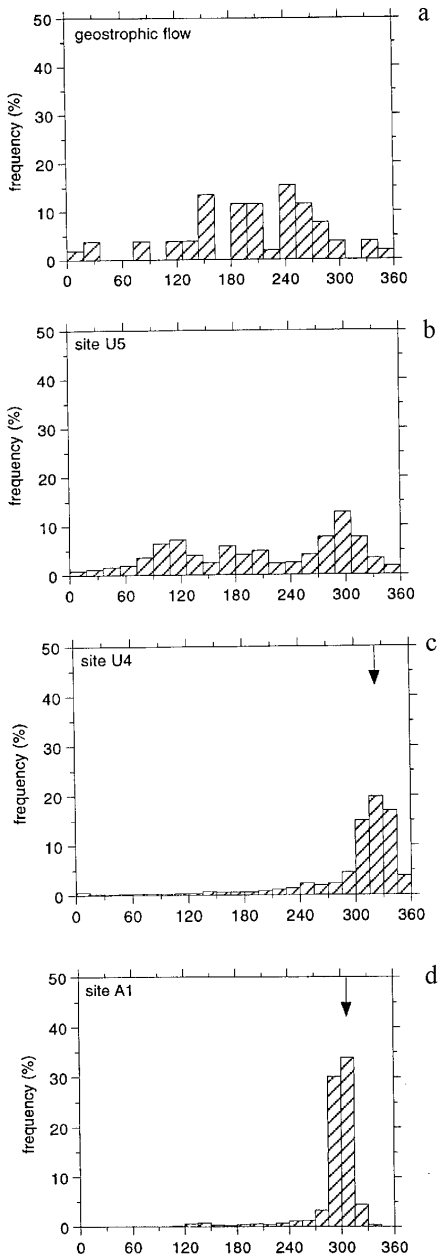

Figure 3. Wind direction frequency distribution during PASTEX for the 500 hPa geostropic flow (a), site U5 (b), site U4 (c) and site A1 (d). The arrow denotes the local downslope direction

3.3. DAILY MEAN VALUES

Daily mean values of pressure, cloudiness, geostrophic and near-surface wind speed and potential temperature are given in Figure 4 a–d. The geostrophic wind vector at 500 hPa was derived from the daily 12 GMT ECMWF analysis. The mountain crests that surround the Pasterze range in elevation between 2500 and 3500 m, the highest peak being the Grossglockner with 3770 m a.s.l. This means that the 500 hPa surface is situated about 1.5–3 km above the crests of the mountains, and the wind at that level should be representative for free atmosphere conditions.

Several weather types could be distinguished during PASTEX. Periods with low pressure (around 8 and 20 July, Figure 4a), are characterised by strong synoptic winds, overcast skies and low temperatures. The potential temperature difference between the various stations on the glacier is small for this weather type, which is indicative of a weak or absent katabatic wind system. During periods with fair weather the potential temperature difference between the stations on the glacier is large: the air is effectively cooled when it flows down the glacier surface, which is an indication of a well developed glacier wind. The wind speed at A1 shows a very steady behaviour with a typical daily mean wind speed of 4 m s^{-1} (Figure 4c), while the wind speed at site U5 usually varies in strength between the 500 hPa wind speed and the wind speed at the glacier tongue. With the aid of balloon soundings at A1 and the geostrophic wind speed at 500 hPa, we are able to estimate the ratio of synoptic pressure gradient to katabatic force, integrated over a layer of certain depth. If we assume a steady state balance within the glacier wind layer between the katabatic force, the synoptic pressure gradient and the sum of interfacial and surface friction, we can write the momentum balance of the ABL as (Van den Broeke et al., 1996a)

$$0 = \frac{g}{\theta_r}\Delta_\theta \frac{\partial h_s}{\partial x} - f v_g - \text{FRICTION}$$

where x points in the downslope direction, U is the characteristic downslope wind speed, Δ_θ is the characteristic temperature deficit of the glacier wind layer compared to the free atmosphere, $\partial h_s/\partial x$ the surface slope (set to -0.087), f the Coriolis parameter (f = 10^{-4} s^{-1}) and v_g the cross slope geostrophic wind speed. For the lowest 10 m of the ABL we found an average temperature deficit Δ_θ = -3.6 K; Figure 5 compares the magnitude of the synoptic pressure gradient $-fv_g$ with the calculated gravity force $(g/\theta_r)\Delta_\theta \partial h_s/\partial x$ for a layer depth H = 10 m, for days on which balloon soundings at 1200 GMT were available. The resulting gravity force is much larger then the synoptic pressure gradient, the average ratio of the two forces being 32 : 1. These results can be compared to those of Stenning et al. (1981), who found a ratio of 7 : 1 on Peyto Glacier. In their study, 65% of the profiles showed a low-level wind maximum (<6 m). At site A1, we found a low-level wind maximum (<13 m) during 75% of the time. For a more thorough

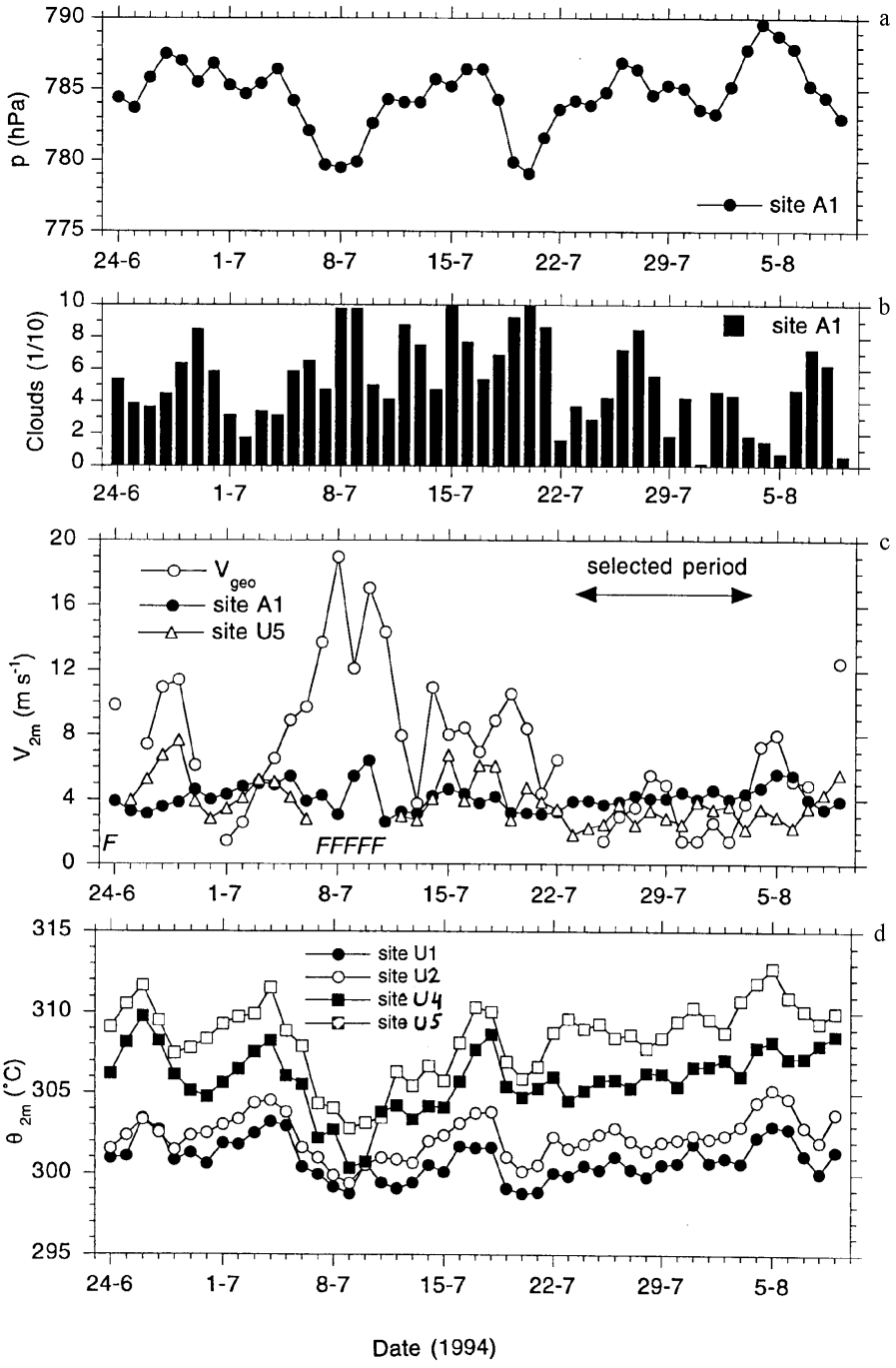

Figure 4. Daily mean values of pressure at A1 (a), cloud cover (b), geostrophic and near surface wind speeds (c) and potential temperature (d) during PASTEX.

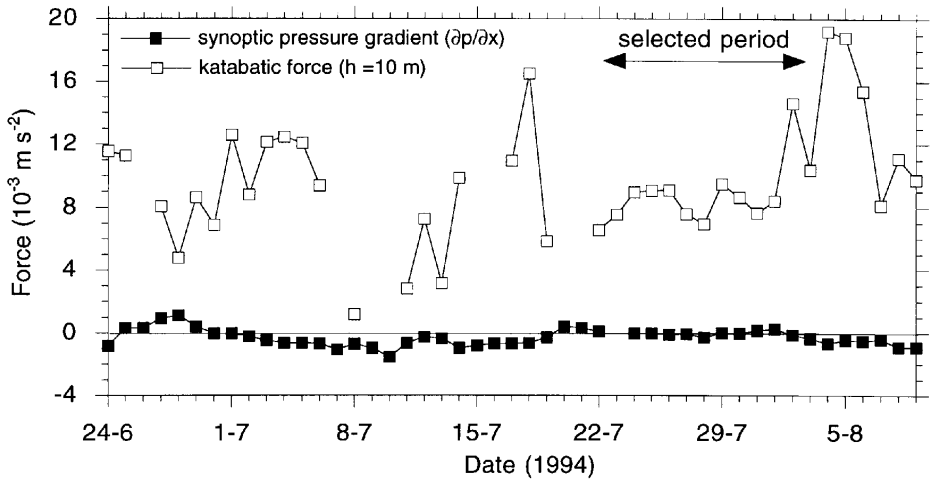

Figure 5. Estimated synoptic pressure gradient force $\partial p/\partial x$ (white dots) and katabatic force for a 10-m deep layer at A1.

treatment of the budgets of momentum, heat and moisture of the katabatic wind layer, the reader is referred to a forthcoming paper (Van den Broeke, 1997b).

3.4. SURFACE ENERGY BALANCE

Table II lists the average energy balance components at sites A1, U2 and U5 for the period 24 June–9 August 1994. In general, the net radiation decreases with elevation due to the increase of the surface albedo and the decrease of incoming longwave radiation (the outgoing longwave radiation is more or less fixed by the melting ice/snow surface). This spatial variation of albedo is typical for valley glaciers during summer (Van de Wal et al., 1992). The turbulent fluxes of sensible and latent heat were calculated from half-hourly mean values of temperature, wind speed and specific humidity at 2 m (Appendix A). Profile data suggest that the aerodynamic roughness length of the melting ice at the glacier tongue (z_0 = 4.4 mm) is almost twice as large as that for the melting snow in the accumulation area (z_0 = 2.3 mm) (W. Greuell, personal communication). Due to the lower temperature, humidity and wind speed at sites U4 and U5, the turbulent fluxes are smaller on the higher parts of the glacier, but they do not vary much with elevation on the glacier tongue. The energy available for melting decreases from 6.2 cm water-equivalents (w.e.) melt per day at site A1 to 2.3 cm w.e. at site U5.

In the stable surface layer, turbulence is suppressed by static stability and generated by wind shear. Because the temperature gradient within the surface layer was generally very large (Figure 2a), we expect that the stability correction strongly reduces the magnitude of the turbulent fluxes of sensible and latent heat. However, according to our calculations, the average stability correction of the turbulent

Table II

Average energy fluxes of net radiation R_{net}, sensible heat flux H, latent heat flux LE, melting energy M, albedo α and friction velocity u_* for the period 24 June–9 August 1994. Amount of missing wind data is given in brackets.

Location	A1	U2 (2%)	U5 (13%)
h_s (m a.s.l.)	2205	2310	3225
R_{net} (W m^{-2})	180	162	65
H(W m^{-2})	51	56	22
LE (W m^{-2})	11	12	1
M (cm w.e. day^{-1})	6.2	5.9	2.3
α	0.20	0.30	0.59
u_* (m s^{-1})	0.25	0.27	0.21

fluxes is only 15% of the neutral flux value. Apparently, the large wind shear in the glacier wind generates sufficient turbulence close to the surface to overcome the stable stratification, i.e., the persistent glacier winds keeps the bulk Richardson number in the surface layer low. The turbulent fluxes of sensible and latent heat make up for 25% of the total melting energy (Table II), so the influence of the glacier wind on the surface energy balance is considerable.

4. Average Diurnal Cycle of the ABL During a Fair Weather Period

A period of 12 days, running from 23 July to 3 August 1994, experienced weak synoptic winds and relatively few clouds (Figure 4b). During this period, the synoptic pressure gradients were especially small (Figure 5) and glacier winds developed favourably: a low level ($<$13 m) wind maximum at A1 was observed for 96% of the time, with an average height of 4.7 m and an average maximum wind speed of 4.5 m s^{-1}. Balloon soundings were performed every three hours during this period in order to obtain a diurnal cycle of the vertical structure of the ABL.

4.1. Diurnal cycle of the vertical structure of the ABL at site A1

Average time-height cross sections of wind speed, wind directional constancy, potential temperature and specific humidity up to 500 m above the glacier surface are presented in Figure 6a–d. Above the glacier wind layer we see the clear signature of a persistent mountain–valley wind circulation (Defant, 1951): a deep layer that flows upslope during daytime (valley wind) and a more shallow layer that flows downslope during the night and merges with the glacier wind (mountain wind) (Figure 6a, positive values denote downslope flow). The glacier wind and the mountain-valley wind system both have a distinctly high directional constancy (Figure 6b), which indicates that both were regular phenomena. The glacier wind

has a daytime maximum in the late afternoon and a secondary maximum just before sunrise. Note that the nightly maximum is most probably *not* due to radiational cooling of the surface, since the ice remains close to the melting point during the night (Section 4.3). It represents the increased downslope mass flux due to the mountain wind, i.e., the gravity flows that develop above the ice-free valley walls that merge with the glacier wind. The main maximum of the glacier wind in the late afternoon is a result of the increased temperature contrast between the glacier surface and the ambient atmosphere and the weakening of the valley wind circulation. The strong temperature and humidity increase above the glacier wind layer at daytime, which is evident from Figure 6c and d, are primarily caused by the advection of warm and humid air from the lower, non-glaciated parts of the valley by the valley wind. This results in an amplitude of the daily cycle of temperature and humidity at several hundreds meters above the glacier that is larger than in the surface layer, which is of course a direct result of the constant temperature of the melting ice surface.

A peculiar feature in Figure 6d is the sudden drying of the ABL in the hours before sunrise. It is suggested that this is caused by enhanced subsidence as a result of merging of the mountain wind with the glacier wind circulation. To quantify this a little bit more, Figure 7 shows the daily cycle of the integrated mass flux at site A1 from the surface to 500 m (positive downslope). During daytime, the upslope transport of air owing to the valley wind by far exceeds the downslope transport of air by the glacier wind, and the net upslope mass flux reaches a maximum of 625 m^3 s^{-1}at 14 local time (LT). During the night, however, the mountain and glacier winds have the same direction, resulting in a net downslope transport of air with a peak value of 300 m^3 s^{-1}at 05 LT. This nocturnal mass divergence will induce downward motion in the ambient atmosphere, so that relatively dry and warm air will be entrained into the ABL.

This process can be quantified if we assume that changes in humidity content of the ABL are forced by changes in the vertical fluxes of moisture at the top (entrainment) and bottom of the ABL, i.e., neglecting the contribution of vertical and horizontal advection. Using first-order closure we can write the entrainment flux at the top of the ABL as $L_v w_e \Delta q$, where L_v is the latent heat of vaporisation, w_e the entrainment velocity and Δq the moisture jump over the entrainment layer. We estimate the entrainment velocity by assuming that the downslope air flux Q in a 500 m deep column at site A1 has been entrained along a trajectory starting at the crest 9 km upstream, where the downslope mass flux is zero: $w_e = \partial Q / \partial x$ then yields an entrainment velocity of 3.3 cm s^{-1} at 0500 LT, and an average value of 1.9 cm s^{-1} for the period between 0200 and 0800 LT. These values can be compared to the estimated entrainment velocity of 0.65 cm s^{-1} for summertime Greenland katabatic winds (Van den Broeke et al., 1994b). If we furthermore assume a specific humidity difference between the free atmosphere and the ABL of Δq = 1 g kg^{-1} (e.g., Figure 2b), the entrainment flux of latent heat at the top of the ABL $L_v w_e \Delta q$ = 47.5 W m^{-2}, which is an order of magnitude larger than the surface flux of

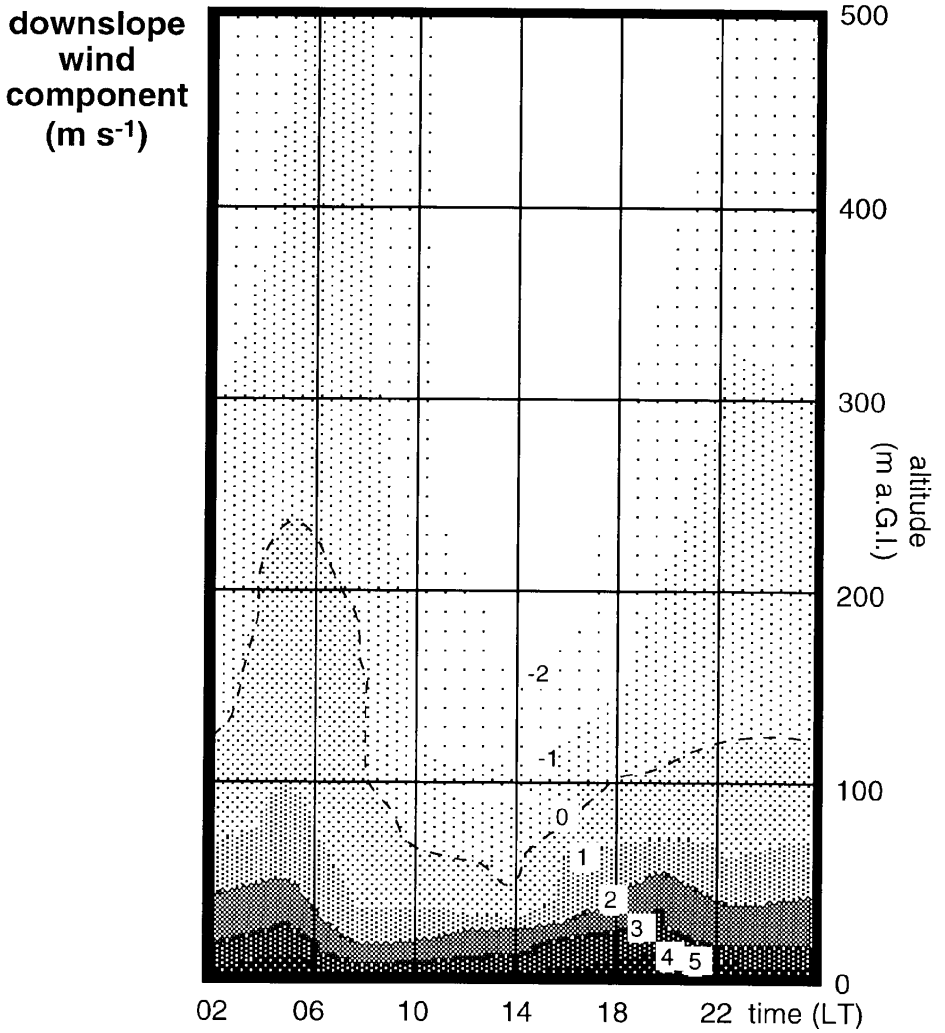

Figure 6. Average diurnal cycle of vertical distribution of downslope wind speed (positive values denote downslope flow) (a), directional constancy (b), potential temperature (c) and specific humidity (d) at A1 during a fair weather period.

latent heat at the same time (see Section 4.3) and sufficiently large to explain the drying of the 500 m thick layer during the night. The sinking motion also tends to slow down the cooling of the ABL air near the surface, because the entrained air is warmer (see next section).

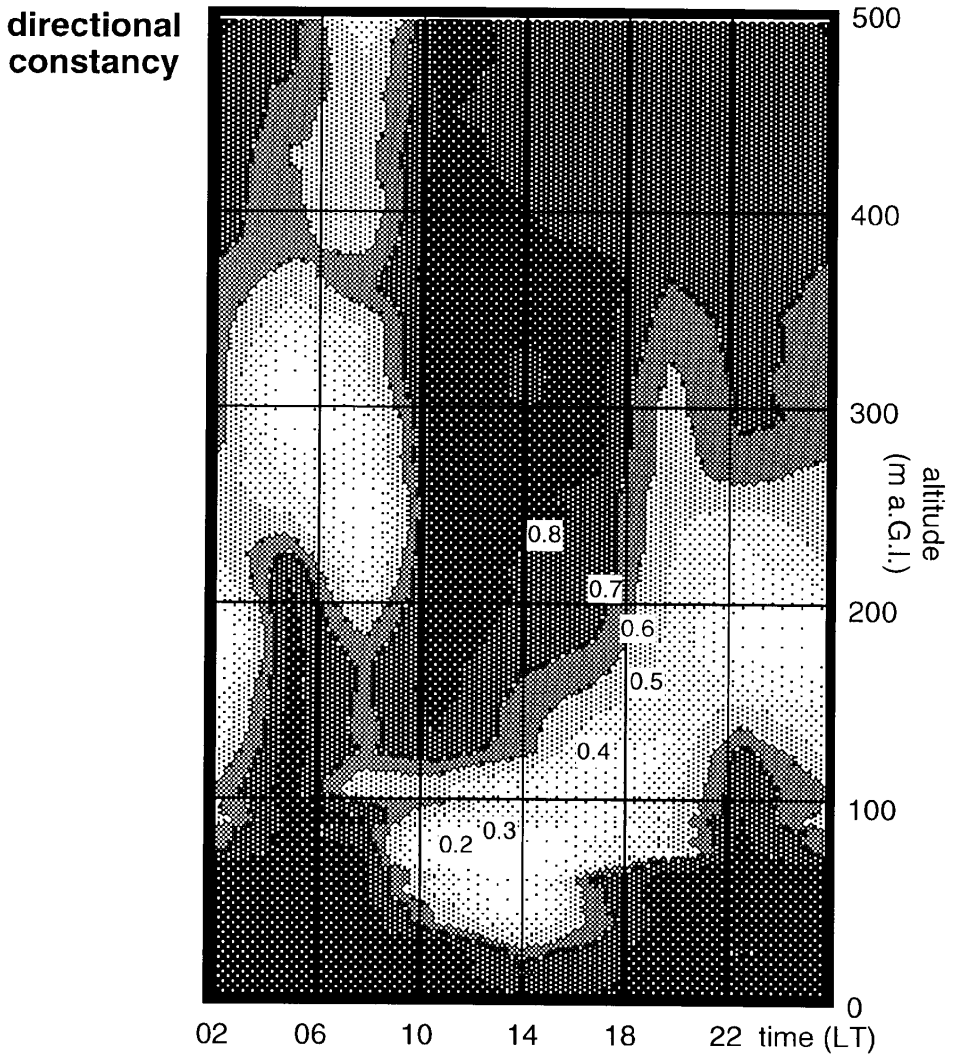

Figure 6b.

4.2. DIURNAL CYCLE OF NEAR-SURFACE VARIABLES DURING A FAIR WEATHER PERIOD

The average diurnal cycles of 2 m potential temperature, specific humidity and wind speed for the same period as discussed in the previous section are presented in Figure 8a–c. Especially at sites above the ice fall the influence of the overlying valley wind can be detected. At sites U4 and U5 the specific humidity strongly increases when the valley wind front passes (Figure 8b). Because the stratification of the surface layer is less strong here, the vertical exchange with the valley wind

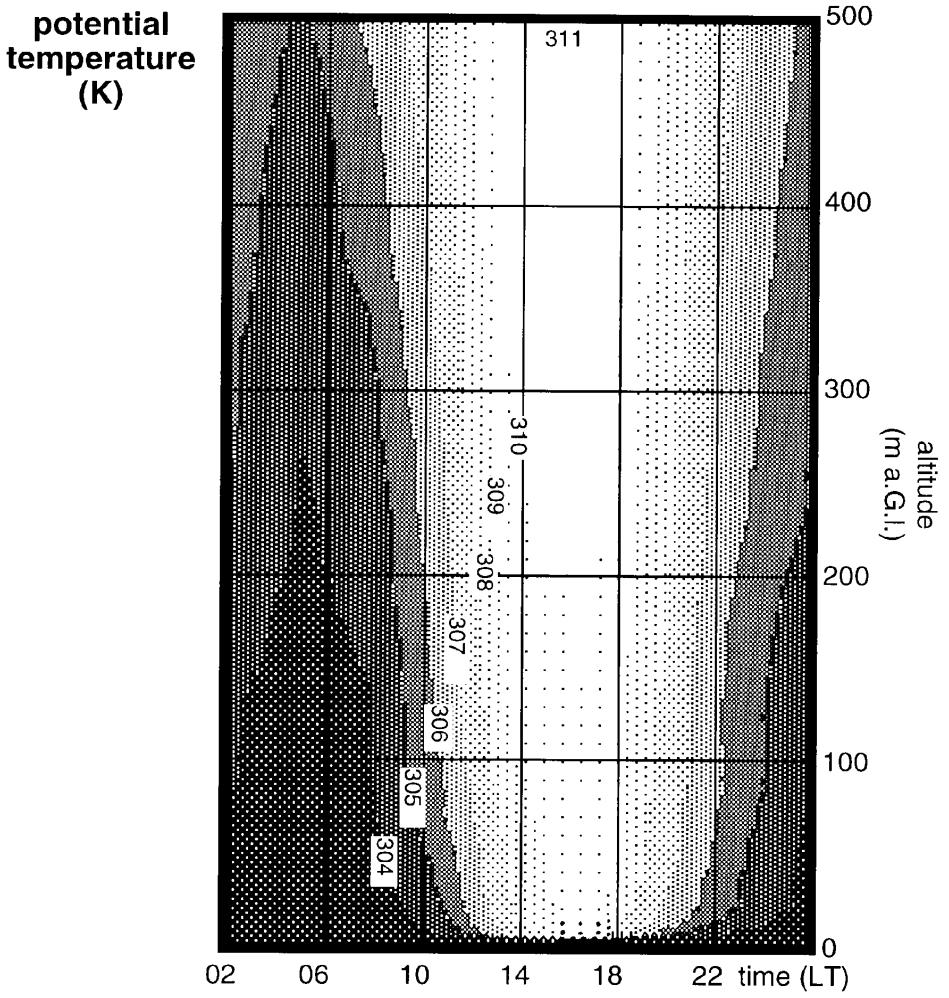

Figure 6c.

at these sites is larger than at the glacier tongue. The time lag of the rise in specific humidity between U4 and U5 in Figure 8b indicates that the valley wind front needs on average 4 hr to cover the 2.5 km distance between these stations. This slow progress can be attributed to the vanishing of the mesoscale horizontal temperature gradient above the glaciated part of the valley; consequently, all further progress of the front is due to advection.

Judging from the decreased downslope wind speed at daytime at U1 and A1 when compared to U2 and U3 (Figure 8c), the valley wind influence on the tongue is larger at the lower stations. This supports the idea that the mesoscale pressure gradient that is associated with the valley wind circulation decreases above the glacier. Only very seldom (less than 1% of the time) does the valley wind actually

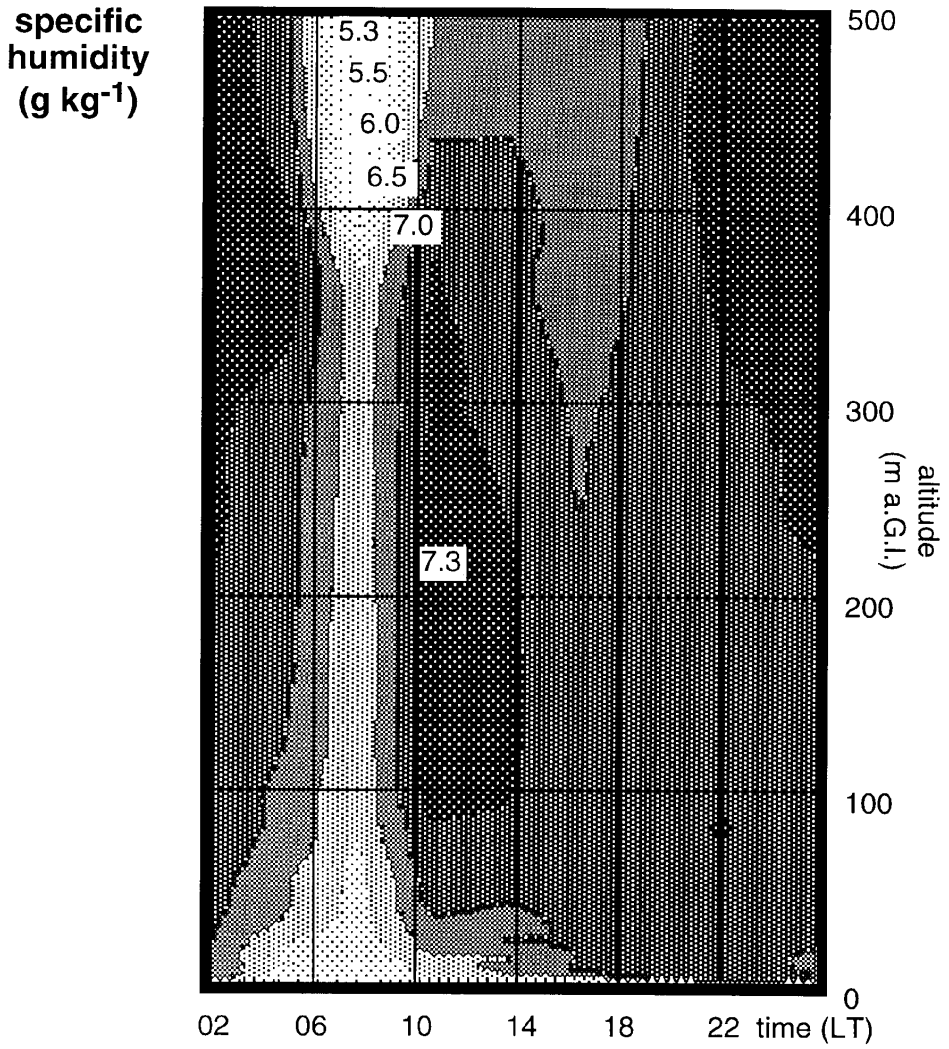

Figure 6d.

penetrate to the glacier surface at the tongue. During the night, when downslope flows from the valley walls merge with the katabatic flow over the glacier, the intensity of the downslope wind at A1 is slightly larger than at U2 and U3, probably because this site has the longest fetch of all the glacier stations. Note the very weak winds at sites U4 and U5 during this period.

A remarkable phenomenon is the strongly reduced diurnal cycle in temperature at site U3 (Figure 8a). Figure 9 shows the average distribution with elevation of potential temperature, as well as the surface (subscript *s*) and background (subscript 0) values; the latter was estimated from balloon soundings. The potential

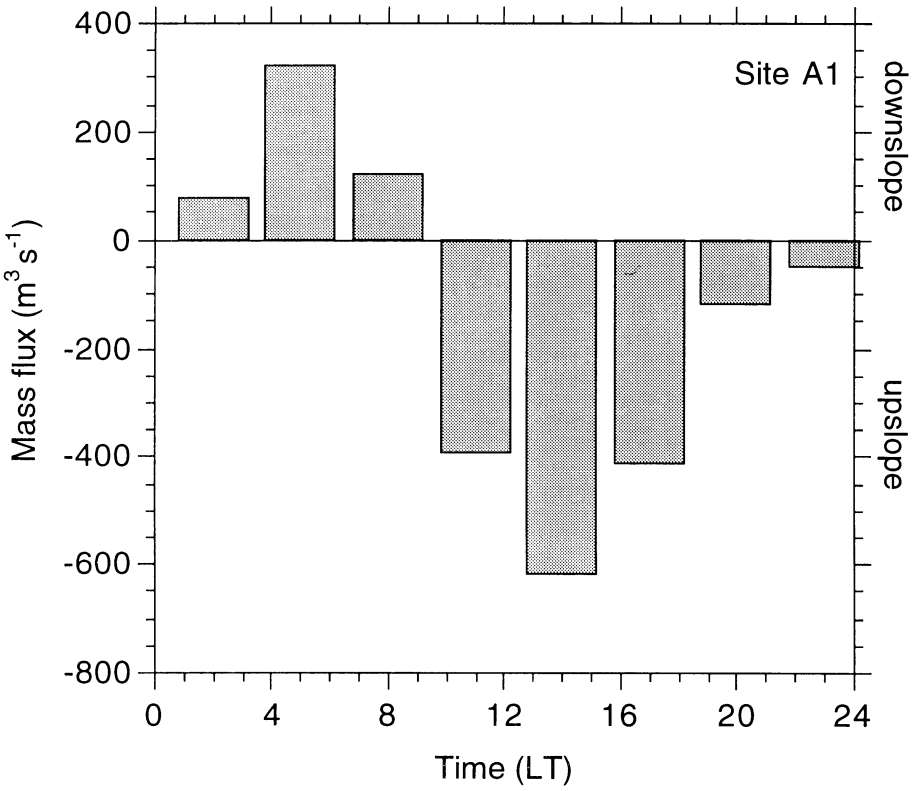

Figure 7. Daily cycle of total downslope mass flux between the surface and 500 m at A1, averaged for a fair weather period.

temperature difference between U3 and U4, situated on either side of the ice fall, vanishes during the night. The most plausible explanation for this is warming at U3 caused by subsidence of the air above the glacier tongue. At site U5, the near surface temperature exceeds the background temperature in the afternoon, probably owing to advection of warm air by the valley wind. Summarising this section, we can state that the mountain–valley wind system has an important influence on surface-layer characteristics in the accumulation area (sites U4 and U5), and also weakly affects near-surface conditions at the tongue.

4.3. DIURNAL CYCLE OF THE ENERGY BALANCE

The average diurnal cycle of the net radiation and the sensible and latent heat fluxes is presented in Figure 10a–c. The diurnal course of turbulent fluxes closely follows the diurnal cycle of the wind speed, because turbulence in the stable ABL is entirely generated by wind shear. The sensible heat flux is, on average, largest at site U3, where the temperature and wind speed have a local maximum. In the accumulation

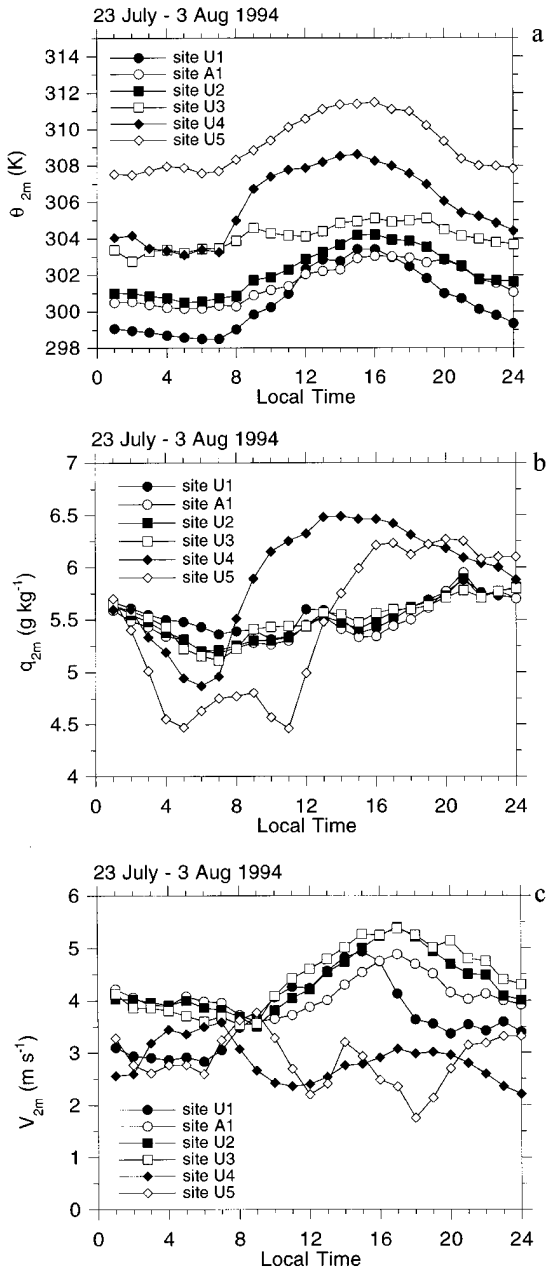

Figure 8. Diurnal cycle of 2 m potential temperature θ_{2m} (a), specific humidity q_{2m} (b) and wind speed V_{2m} (c), averaged for a fair weather period.

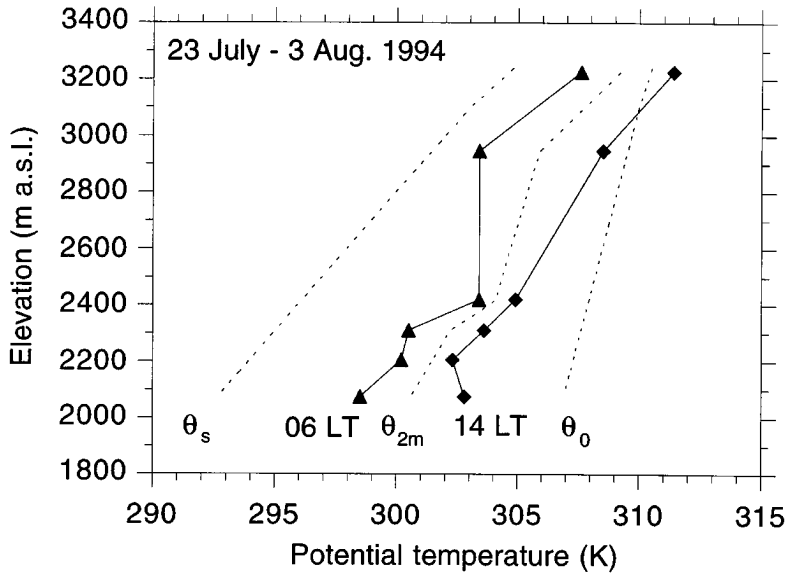

Figure 9. Average distribution of 2 m potential temperature θ_{2m} (middle dashed line) for a fair weather period at night and in the afternoon (solid lines) and background (subscript 0) and surface (subscript s) values (left and right dashed lines). The background potential temperature profile was estimated from balloon soundings.

zone there is evaporation during the night and weak condensation during daytime. This variation is caused by the diurnal cycle of the valley wind advecting warm and humid air by day and causing drying of the atmosphere at night, as discussed in the previous section. On the glacier tongue, condensation is a day-round feature, with a minimum at night, which is associated with the drying of the air column and the lower wind speeds. At A1, the sensible and latent heat fluxes compensate for the longwave radiation loss of the surface at night, so the surface temperature will remain close to the melting point. At site U2 and U5, where the net longwave radiation during the night is more negative, we expect frequent refreezing of the ice/snow surface. At daytime, the net radiation dominates the energy balance at all sites.

5. Conclusions

The observations performed during PASTEX show that persistent glacier winds determine the vertical and horizontal structure of the ABL above the Pasterze glacier in summer. These winds are forced by gravity, and they are hardly influenced by the synoptic-scale pressure gradients or entrainment of air from aloft. Glacier winds effectively generate turbulence in the stably stratified surface layer. They are especially well developed during periods with weak synoptic flow and strong

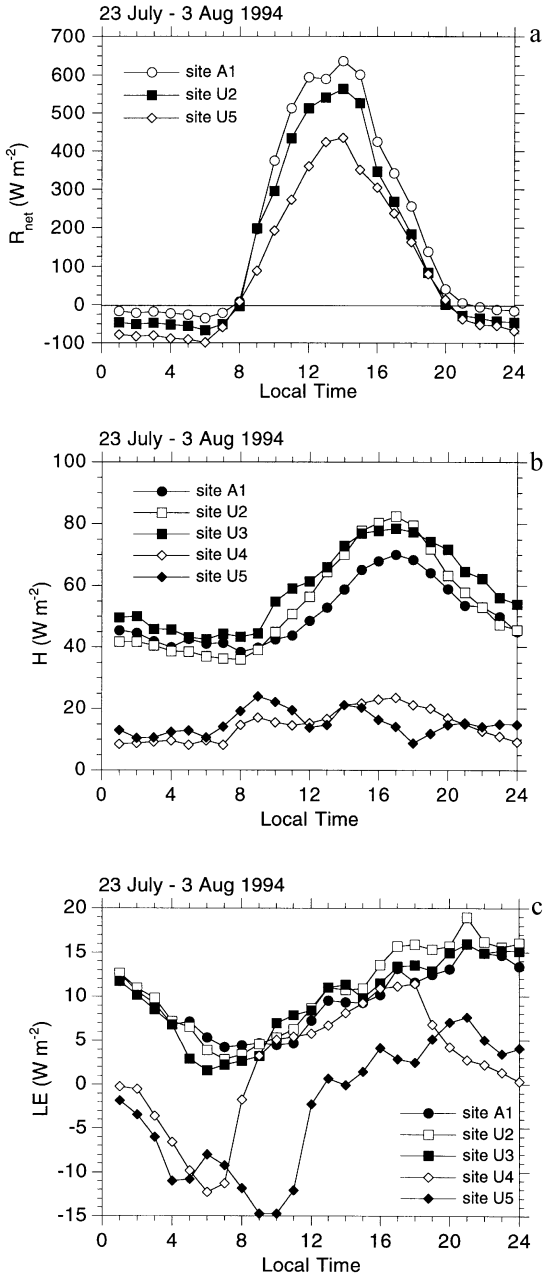

Figure 10. Diurnal cycle of net radiation R_{net} (a), sensible heat flux H (b) and latent heat flux LE (c), averaged for a fair weather period.

insulation and enhance the melt rates. At the lower parts of the glacier the turbulent flux of sensible and latent heat make up for roughly 25% of the melting energy. Higher up in the accumulation zone, where the temperatures are lower and the surface-layer stratification not so stable, the ABL is more sensitive to external forcing, such as the valley wind that advects moist and warm air from the valley floor. The net radiation at the surface as well as the turbulent fluxes are significantly smaller in the accumulation zone than at the glacier tongue. The pronounced mass flux divergence within the lower parts of the atmosphere during the night, caused by the combined effect of the glacier and mountain wind, produces drying and warming of the ABL air.

Acknowledgements

All participants of PASTEX are thanked for their help during the expedition, especially those who performed the nightly balloon soundings. W. Greuell performed the initial data reduction and C. Reijmer and I. Struijk calculated the geostrophic flow from ECMWF analysis. P. G. Duynkerke, J. Oerlemans and R. S. W. van de Wal are thanked for interesting and stimulating discussions. The data of the mast at site A1 were kindly provided by P. Smeets and H. F. Vugts from the Free University of Amsterdam.

Appendix A: Calculation of the Surface Fluxes

To calculate the turbulent fluxes from half-hourly values of wind speed, temperature and specific humidity at 2 m over a melting glacier, we followed the approach of Munro (1989). We assume that the melting ice surface remains at 0 °C, while the air just above it is saturated with respect to water. Based on profile measurements, a value of 4.4 mm was adopted for the aerodynamic roughness length z_0 over ice (site A1, U2 and U3) and 2.3 mm over snow (U4 and U5). The roughness length for heat and moisture z_h is determined using the expression proposed by Andreas (1987). This expression relates z_h to z_0 as a function of the roughness Reynolds number Re = $u_* z_0 v^{-1}$, where ν is the kinematic viscosity of air. Data collected by Bintanja and Van den Broeke (1995a), Munro (1989) and Kondo and Yamazawa (1986) confirmed the general shape of Andreas' expression for a wide range of roughness Reynolds numbers (Bintanja and Van den Broeke, 1995b). The stability corrections given by Duynkerke (1991) are used; for moderately stable conditions ($zL^{-1} \ll 1$, where L is the Obukhov length) these expressions yield good results, and are quite similar to those proposed by Högström (1987).

References

Andreas, E. L.: 1987, 'A Theory for the Scalar Roughness and the Scalar Transfer Coefficients Over Snow and Sea Ice', *Boundary-Layer Meteorol.* **38**, 159–184.

Bachmann, R. C.: 1978, *Gletscher der Alpen*, Hallwag Verlag, Bern und Stuttgart.

Bintanja, R. and van den Broeke, M. R.: 1995a, 'The Surface Energy Balance of Antarctic Snow and Blue Ice', *J. Appl. Meteor.* **34**, 902–926.

Bintanja, R. and van den Broeke, M.R.: 1995b, 'Momentum and Scalar Transfer Coefficients Over Aerodynamically Smooth Antarctic Surface', *Boundary-Layer Meteorol.* **78**, 89–111.

Defant, F.: 1951, 'Local Winds, in T. F. Malone (ed.), *Compendium of Meteorology*, American Met. Soc., Boston, pp. 655–672.

Duynkerke, P. G. and van den Broeke, M.R.: 1994, 'Surface Energy Balance and Katabatic Flow Over Glacier and Tundra During GIMEX-91', *Global Planetary Change* **9**, 17–28.

Duynkerke, P. G.: 1991, 'Radiation Fog: A Comparison of Model Simulation with Detailed Observations', *Mon. Wea. Rev.* **119**, 324–341.

Greuell, W. et al.: 1994, PASTEX Field Report, IMAU, Utrecht University. (Can be obtained from IMAU, PO Box 80.005, 3508 TA Utrecht, The Netherlands.)

Högström, U.: 1987, 'Non-dimensional Wind and Temperature Profiles in the Atmospheric Surface Layer: A Re-evaluation', *Boundary-Layer Meteorol.* **42**, 55–78.

Hoinkes, H. C.: 1954, 'Die Einfluss des Gletscherwindes auf die Ablation', *Z. Gletscherkunde Glazialgeologie* **3**(1), 18–23.

Holmgren, B.: 1971, 'Climate and Energy Exchange on a Sub-polar Ice Cap in Summer', *Arctic Institute of North America, Devon Island Expedition 1961–1963*, Part C: *On the Katabatic Winds on the NW Slope of the Ice Cap, Variation of the Surface Roughness*, Meteorological Dept. Uppsala University, No. 109, 43 pp.

Kodama, Y., Wendler, G. and Ishikawa, N.: 1989, 'The Diurnal Variation of the Boundary Layer in Summer in Adélie Land, Eastern Antarctica', *J. Appl. Meteorol.* **28**, 16–24.

Kondo, J. and Yamazawa, H.: 1986, 'Bulk Transfer Coefficient Over a Snow Surface', *Boundary-Layer Meteorol.* **34**, 123–135.

Kuhn, M.: 1978, 'Die Höhe des Geschwindigkeitsmaximums im Gletscherwind als Parameter des Wärmehaushalts', Zentralanstalt für Meteorologie und Geodynamik in Wien. Publikation 228, 69/1-69/8.

Martin, S.: 1975, 'Wind Regimes and Heat Exchange on Glacier de Saint-Sorlin', *J. Glaciol.* **14**, 91–105.

Munro, D. S.: 1989, 'Surface Roughness and Bulk Heat Transfer on a Glacier: Comparison with Eddy Correlation', *J. Glaciol.* **35**, 343–348.

Munro, D. S. and Davies, J. A.: 1977, 'An Experimental Study of the Glacier Boundary Layer Over Melting Ice', *J. Glaciol.* **18**, 425–436.

Munro, D. S. and Davies, J. A.: 1978, 'On Fitting the Log-Linear Model to Wind Speed and Temperature Profiles Over a Melting Glacier', *Boundary-Layer Meteorol.* **15**, 423–437.

Oerlemans, J.: 1994, 'Quantifying Global Warming from the Retreat of Glaciers', *Science* **264**, 243–245.

Oerlemans, J. and Fortuin, J. P. F.: 1992, 'Sensitivity of Glaciers and Small Ice Caps to Greenhouse Warming', *Science* **258**, 115–117.

Ohata, T.: 1989a, 'The Effect of Glacier Wind on Local Climate, Turbulent Heat Fluxes and Ablation', *Z. Gletscherkunde Glazialgeologie* **25**, 49–68.

Ohata, T.: 1989b, 'Katabatic Wind on Melting Snow and Ice Surfaces (I): Stationary Glacier Wind on a Large Maritime Glacier', *J. Met. Soc. Japan* **67(1)**, 99–112.

Parish, T. R. and Waight, K. T.: 1987, 'The Forcing of Antarctic Katabatic Winds', *Mon. Wea. Rev.* **115**, 2214–2226.

Schwabl, W. and Tollner, H.: 1938, 'Vertikalbewegungen der Luft über einem Gletscher', *Meteorol. Z. 1938*, 61–64.

Stenning, A. J., Banfield, C. E., and Young, G. J.: 1981, 'Synoptic Controls over Katabatic Layer Characteristics Above a Melting Glacier', *J. Climatol.* **1**, 309–324.

Tollner, H.: 1931, 'Gletscherwinde in den Ostalpen', *Meteorol. Z. 1931*, 414–421.

Tollner, H.: 1935, 'Gletscherwinde auf der Pasterze', *Jahresbericht des Sonnblickvereines 1935*, Wien, pp. 38–54.

Tollner, H.: 1952, *Wetter und Klima im Gebietes des Grossglockners*, Klagenfurt.

Van de Wal, R. S. W., Oerlemans, J., and van der Hage, J. C.: 1992, 'A Study of Ablation Variations on the Tongue of Hintereisferner, Austrian Alps', *J. Glaciol.* **38**, 319–324.

Van den Broeke, M. R., Duynkerke, P. G. and Oerlemans, J.: 1994a, 'The Observed Katabatic Flow at the Edge of the Greenland Ice Sheet During GIMEX-91', *Global Planetary Change* **9**, 3–15.

Van den Broeke, M. R., Duynkerke, P. G., and Henneken, E. A. C.: 1994b, 'Heat, Momentum and Moisture Budgets of the Katabatic Layer Over the Melting Zone of the West-Greenland Ice Sheet in Summer', *Boundary-Layer Meteorol.* **71**, 393–413.

Van den Broeke, M. R. and Bintanja, R.: 1995, 'Summertime Atmospheric Circulation in the Vicinity of a Blue Ice Area in Queen Maud Land, Antarctica', *Boundary-Layer Meteorol.* **72**, 411–438.

Van den Broeke, M. R.: 1996, 'The Atmospheric Boundary Layer Over Ice Sheets and Glaciers', Ph.D. Thesis, Utrecht University, The Netherlands. (Can be obtained from the author.)

Van den Broeke, M. R.: 1997a, 'A Bulk Model of the Atmospheric Boundary Layer for Inclusion in Mass Balance Models of the Greenland Ice Sheet', *Z. Gletscherkunde Glazialgeologie*, **33**(1), 73–94.

Van den Broeke, M. R.: 1997b, 'Momentum, Heat and Moisture Budgets of the Katabatic Wind Layer Over a Mid-Latitude Glacier in Summer', *J. Appl. Meteorol.*, in press.

Warrick, R. and Oerlemans, J.: 1990, 'Sea Level Rise, in J. T. Houghton et al. (eds.), *Climate Change*, The IPCC Scientific Assessment, Cambridge University Press, pp. 257–282.

Wendler, G., André, J. C., Pettré, P., Gosink, J., and Parish, T.: 1993, 'Katabatic Winds in Adélie Coast', in D. H. Bromwich and C. R. Stearns (eds.), *Antarctic Meteorology and Climatology, Studies Based on Automatic Weather Stations*, Antarctic Research Series 61, American Geophysical Union, pp. 23–46.